**JURNAL SAINS MATERI INDONESIA (JUSAMI)**
ISSN: 1411-1098 (print), 2614-087X (online)
VOL. 23, ISSUE 2, April 2022
DOI: https://doi.org/10.17146/jsmi.2022.23.5.6427

**ORIGINAL ARTICLE**

# The Advanced Electric Field from Quad-Electrode Mode for Blood Cancer Cells Trapping: Simulation Study

M. Firdhaus[1], U. Farahdina[1], V. Z Zulfa[1], A. R. H. Tahier[2], M. Haekal[1], Endarko[1], Darsono[3], A. Rubiyanto[1,*] and Nasori[1]

[1] Laboratory of Medical Physics and Biophysics, Department of Physics, Institut Teknologi Sepuluh Nopember, Kampus ITS, Surabaya, 60111
[2] Automation Engineering Technology, Vocational School, Diponegoro University, Semarang, 50275
[3] Research Center Accelerator Energy, National Research and Innovation Agency

**ABSTRACT** – Blood cancer is a disease caused by the rapid cleavage of white blood cells (WBC), which increases in the human circulatory system. Furthermore, based on the original nature of WBC during cleavage, which is the same as ionic bonds, electric field filtering, and trapping is used to treat leukemia patients. The electric field generated by the electrode with an AC voltage source plays a role in the migration of the WBC to high electric field intensity. The Quad-electrode field distribution is conducted using the Finite Element Method (FEM), and an electric field gradient analysis is conducted to determine the effectiveness of each coordinate system. According to the simulation results, the second model with an input voltage of 0.68 V has the highest intensity of electric field distribution, with an effective depth at Z = 30 mm, and the best coordinate along the X-axis and Y-axis are 30 mm. In conclusion, the center of the Quad-electrode system center is the best location for placing filters and trapping leukocytes by utilizing electric field distribution on the electrode system for the development of blood cancer biomedical therapy technology.

**ARTICLE HISTORY**
Received: 10 August 2021
Revised: 26 April 2022
Accepted: 9 May 2022

**KEYWORDS**
Blood cancer,
Filtering,
Electric field,
Dielectrophoresis,
Biomedical

## INTRODUCTION

Cancer disease is not easily detected at the beginning of its symptoms, hence the number of patients continues to increase every year [1]. In medical science, there are 3 main types of blood cancer, namely, Leukemia, Lymphoma Myeloma, and Plasma Cell disorders [2]. Leukemia is a metastatic and dangerous disease in the blood-producing organs (bone marrow), and lymph system, which results in increased and proliferative problems of the white blood cells. The division of the white blood cell division in leukemia patients occurs very quickly, resulting in a high concentration of blast cells in the blood [3]. Furthermore, the high levels of blast cells cause many problems in the body and need to be reduced, hence normalizing the blood components in the bloodstream. The reduction is achieved by filtering the blast cells [4]–[9] because they are larger in size than others (eg, red blood cells and platelets) [10]. Additionally, the filtration is continued by trapping the cells using the dielectrophoresis method, to direct the blast cells to the filter area and trap them there, hence avoiding the contamination of the filtered blood [11]–[14]. In addition to filtration, the blast cells are also being damaged using an AC electric field on the cell membrane [15], [16].

Currently, the methods used in the treatment of leukemia are chemotherapy, radiotherapy, and stem cell transplantation, which have high costs and few side effects on normal cells. Therefore, as an alternative, the filtration and trapping of blast cells are being used. The electric field, apart from being used to trap blast cells, has the ability to penetrate the membrane and affect the cell as long as it divides [17]. At low frequencies below 1 kHz, an alternating electric field stimulates the tissue through a membrane depolarization mechanism [18]. In addition, it stimulates bone growth and accelerates fracture healing [19]. Meanwhile, at high frequencies (above MHz), network heating becomes dominant due to dielectric loss. This effect becomes stronger with an increase in the frequency, field intensity, and tissue dissipation factor [20], and at intermediate frequencies between (10 kHz to MHz), the alternating electric fields rapidly create nerve and muscle stimulation as well as dielectric loss, then reduce heating. It is being observed that low to medium intensity [20] and alternating electric fields with a frequency of 100 kHz or above [21] have no significant biological effect. Therefore, in this simulation, the frequency of 100 kHz is used as the input parameter of the electric field.

The inhomogeneous cell motion in an electric field has been studied and it is known as electrophoresis [22]. In addition, there are two types of electrophoresis, namely, positive and negative. Positive electrophoresis occurs when the particle moves towards an area of the high electric field intensity, while negative occurs when the particle moves towards a weak electric field intensity [13]. Huang and Pethig [23], designed an electrode capable of generating negative electrophoresis, resulting in 4 electrodes that are used to produces negative and positive electrophoresis.

Different electrode arrangements are capable of produces several electric field distributions, which however affect the movement of the suspended particles. Previously, the distribution of the electric field with 2 electrodes in the blood medium was conducted, resulting in the maximum intensity in the area near the electrode (2 areas) and the lowest intensity in the middle of the electrode spacing [24]. Existing research only utilizes electric fields for the treatment of tumors in the head and has not utilized electric fields for clinical leukemia therapy. The electric field distribution simulation for the

***CORRESPONDING AUTHOR** | A. Rubiyanto | ✉ arubi@physics.its.ac.id

treatment of leukemia that already exists utilizes the biological parameters of mice by using the opposite electrode configuration only.

The electric field used for the treatment of leukemia can be developed using a 4-electrode configuration. The addition of 4 electrodes was carried out to increase the homogeneity of the electric field and optimize the dielectrophoretic force to shift blast cells particles closert to the high intensity field areas to trap them. In addition, variations in the arrangement of the electrode polse were carried out on a 4 electrode system. Numerical simulation of the electric field were analysed to obtain optimum electric field gradients at input voltage of 0.34 V and 0.68 V.

## EXPERIMENTAL METHOD

### Model Schematic

The schematic model of the simulation starts by taking blood from the body and placing it in a chamber of the dimensions 60 × 60 × 60 $mm^3$ as shown in Figure 1, which was selected to simplify the system. Furthermore, The blood is given an AC signal with a voltage amplitude of 0.34 V and 0.68 V and the phase difference at each electrode of $\pi/4$. In this study, variations in the arrangement of electrodes and blood medium are conducted, and In model 1, the poles of the same electrode are arranged close to each other. While in model 2, the poles of the same electrode are arranged to face each other. In Figure 1, the blue color in the container indicates a positive voltage while the gray shows a negative voltage.

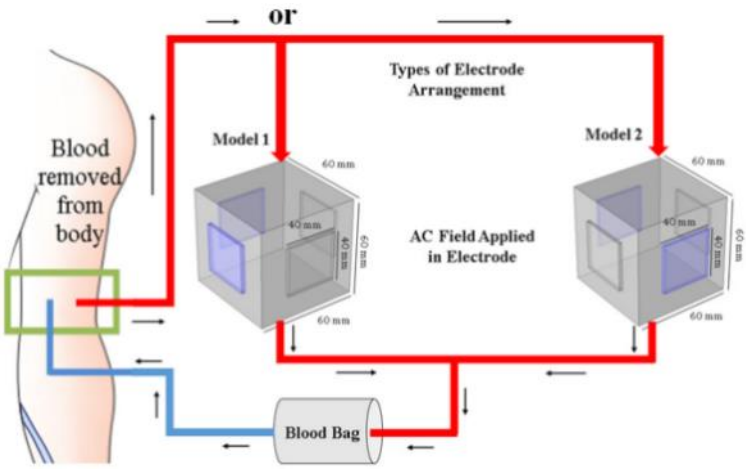


**Figure 1.** The schematic model of the simulation. The blood is removed from the body and placed in a container given AC electric fields with an electrode arrangement such as model 1 (left) and model 2 (right). The process is continued by collecting the blood in a bag and trans-fused it into the body.

The area between the electrodes represents a medium filled with normal blood, B lymphocytes, and T lymphocytes. Furthermore, the physical parameters used are homogeneous and isotropic electrical properties (relative permittivity) for normal blood, B lymphocytes, and T lymphocytes with values of 5120, 5063, and 4650 respectively and at a frequency of 10 kHz [25], [26]. The electrode is given a positive and negative minimum voltage of 0.34 V which is used as a threshold for leukocyte oxidation [27] and a voltage of 0.68 V is used as a variation.

### Simulation Conditions

The electric field distributions are computed using COMSOL Multiphysics 5.4 software, which is capable of solving partial differential equations (PDP) following physical laws using the finite element (FEM) method. In this case, the electric field distribution with the COSMOL electrostatic (es) module is determined using the following equation:

$$\nabla D = \rho V \tag{1}$$

$$E = \frac{D}{\varepsilon_0 \varepsilon_r} \tag{2}$$

$$E = -\nabla V \tag{3}$$

where D is the electric displacement, $\rho$ is the charge density, $\varepsilon_0$ and $\varepsilon_r$ are the vacuum and relative permittivity of the medium, and V is the electric potential. The Dirichlet boundary condition allows the application of a constant scalar potential (i.e., input voltage) to the surface of the model. In addition, the electric field distribution is identified by 2-dimensional analysis on the XY cross-sectional plane with a variation of the Z-coordinate (enclosed and not covered by electrodes). Then, the electric field is plotted along the Z-coordinate with various points in the XY plane to analyze electric field strength with a squared gradient. Subsequently, the electric field is plotted along the fixed X & Y coordinate.

## RESULT AND DISCUSSION

The electric field distribution is compared to the variation and arrangement of the medium as well as the electrode respectively (model 1 and 2), and the input voltage. This arrangement determines the electric field distribution in the system, which is compared to discover a homogeneous model.

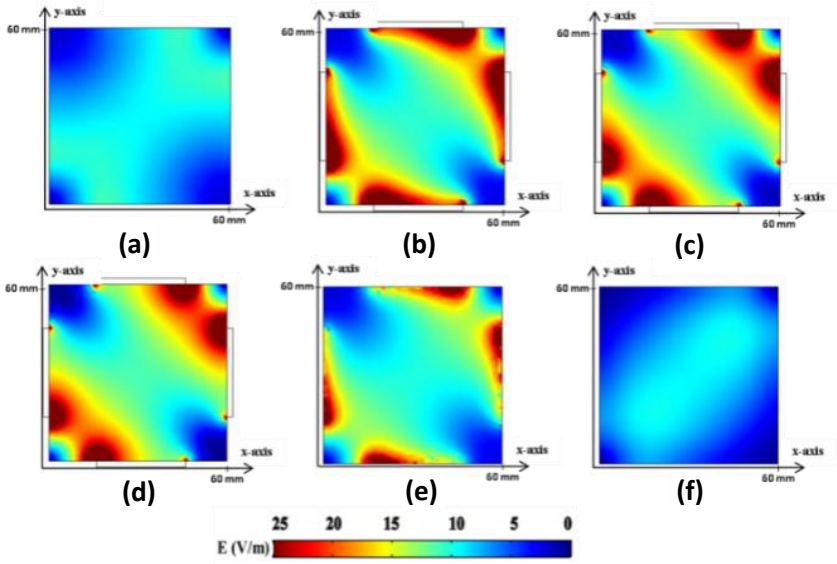


**Figure 2.** Electric field distribution for model 1: (a) Z = 10 mm, (b) Z = 20 mm, (c) Z = 30 mm, (d) Z = 40 mm, (e) Z = 50 mm, and (f) Z = 60 mm

The electric field distribution in model 1 has been plotted on the cross-section of the XY plane by varying the Z-coordinate with an interval of 10 mm as shown in Figure 2. In general, each increase in the Z value indicates a symmetric distribution, whereby the area outside the electrode scope (Z <10 mm and Z > 50 mm) has a low intensity of electric field distribution. Meanwhile, the area inside the electrode range (20 mm < Z < 40 mm) has higher intensity of electric field distribution, and the center area (Z = 30 mm) has the maximum electric field intensity distribution. Furthermore, the distributions for model 2 as shown in Figure 3 have a similar trend to model 1. The area outside the electrode scope (Z < 10 mm and Z > 50 mm) has a low intensity of electric field distribution, while the area inside the electrode (20 mm < Z < 40 mm) has higher electric field intensity distribution, and the area around the center (Z = 30 mm) has the maximum electric field intensity distribution.

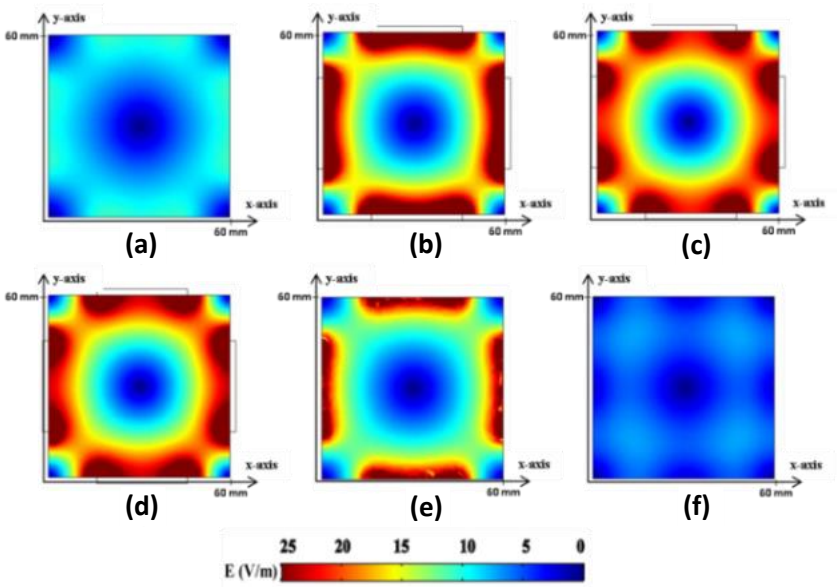


**Figure 3.** Electric field distribution for model 2: (a) Z = 10 mm, (b) Z = 20 mm, (c) Z = 30 mm, (d) Z = 40 mm, (e) Z = 50 mm, and (f) Z = 60 mm

After determining the electric field distribution of the two models, the results of the area outside, and especially in the center of the electrode (Z = 30 mm) are compared. In model 1, high intensity occurs in the electrode area with opposite poles, where it has only 4 high-intensity points, and it is not very intense in the middle area of the XY plane, it has a not very high intensity. While in model 2, the high-intensity is on the edge with 8 points, and in the center of the XY plane, it has the smallest value. Due to several points of high intensity, model 2 has better distribution than model 1, hence it is selected for medium and input voltage variations.

Additionally, model 2 has a unique distribution, where the central area of the XY plane has a minimum intensity, and it is used under certain conditions to protect the central area occupied by sensitive tissues against electric fields. Bioparticles are sensitive to the presence of electric fields [28] when hitting inappropriately, hence causing damage [29]. The sensitivity usually depends on the effect of Joule heating and the intensity of the electric field, therefore model 2 is used for minimizing the intensity in sensitive tissues located in at the middle (such as bone marrow as a place for new blood cells formation).

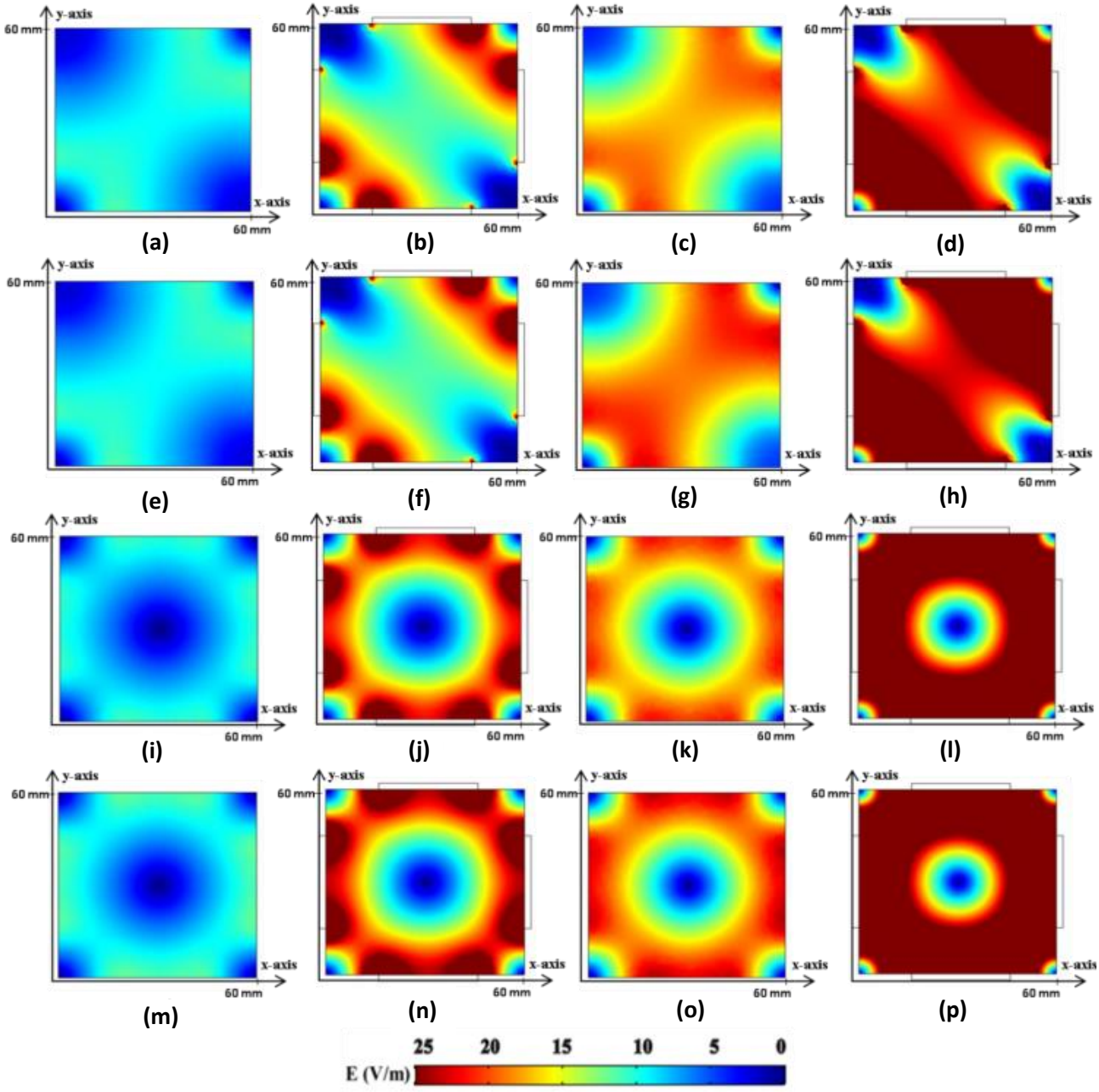


**Figure 4.** The Electric field distribution of the B lymphocytes (top) and T lymphocytes (bottom) with variations in the input voltage: (a) Model 1 with 0.34 V in B lymphocytes outside the electrode scope, (b) Model 1 with 0.34 V in B lymphocytes in the center of the electrode, (c) Model 1 with 0.68 V in B lymphocytes outside the electrode scope, (d) Model 1 with 0.68 V in B lymphocytes in the center of the electrode, (e) Model 2 with 0.34 V in T lymphocytes outside the electrode scope, (f) Model 2 with 0.34 V in T lymphocytes in the center of the elec-trode, (g) Model 2 with 0.68 V on T lymphocytes outside the electrode scope, and (h) Model 2 with 0.68 V in T lymphocytes in the center of the electrode.

In the medium and input voltage variations, data samples are obtained from the area outside the scope (Z = 10 mm) and in the center (Z = 30 mm) of electrodes of the B and T lymphocytes medium. Figure 4 shows the electric field distribution using the electrode arrangement model 2 on B and T lymphocytes medium with an input voltage of 0.34 V and 0.68 V. B, and T lymphocytes have different permittivity values, but at an input voltage of 0.34 V, there is no significant difference between the two. However, by increasing the voltage to 0.68 V, the intensity in the T-lymphocyte medium is higher than that of the B-lymphocyte. The differences are indicated by a red color in the distribution of the T-lymphocyte medium. This is because the high voltage increases the charge accumulation, then the combination of many charges creates a large electric field [30]. The increase in the field value of T lymphocytes is caused by the small permittivity. The smaller the permittivity value, the easier the electric field to align its orientation, then the electric field will be greater [31].

Model 2 has a better and unique electric field distribution than model 1. Also, it has a minimum intensity at the center that is useful in the future. Therefore, to determine the distribution at the XY point along the Z-axis which represents the container depth, a 1D plotting is being conducted in the XY plane with variations in the Z-axis distance. The XY point is taken at the coordinates (10, 10), (10, 30), (10, 50), (30, 10), (30, 30), (30, 50), (50, 10), (50, 30), and (50, 50). Meanwhile, the 1D graph of the electric field along the Z-axis can be used to analyze the gradient by looking at its slope.

The point at the center of the Z axis of the electrode placement, which is at a position of 30 mm, indicates the minimum electric field value, while the point very close to the edge of the electrode indicates the maximum electric field value. The electric field value is obtained from the calculation of the electric field value at each point along the XY axis from the simulation results as shown in Figure 5. There is a change in the electric field gradient to a fairly large position in the area around the center of the Z axis. and the optimum electric field gradient at that position occurs due to the destructive interference of the AC electric field generated from each electrode placed as shown in Figure 1.

The electric field gradient along the Z-axis is shown in Figure 5 (a), (b), (c), and (d) for model 2 and Figure 5 (e) and (f) for model 1. The Z-axis is optimally obtained at Z = 30 mm as shown in Figure 5, where the maximum electric field appears at that point. In model 2, there are 4 points with a maximum distribution in the XY plane, namely (10.10), (10.50), (50.10), and (50.50) with values of 43 V/m, 43 V/m, 45 V/m, and 45 V/m respectively. The gradient is observed from Z = 0 mm to Z = 30 mm. At Z = 30 mm and above, it shows symmetry with a negative gradient value.

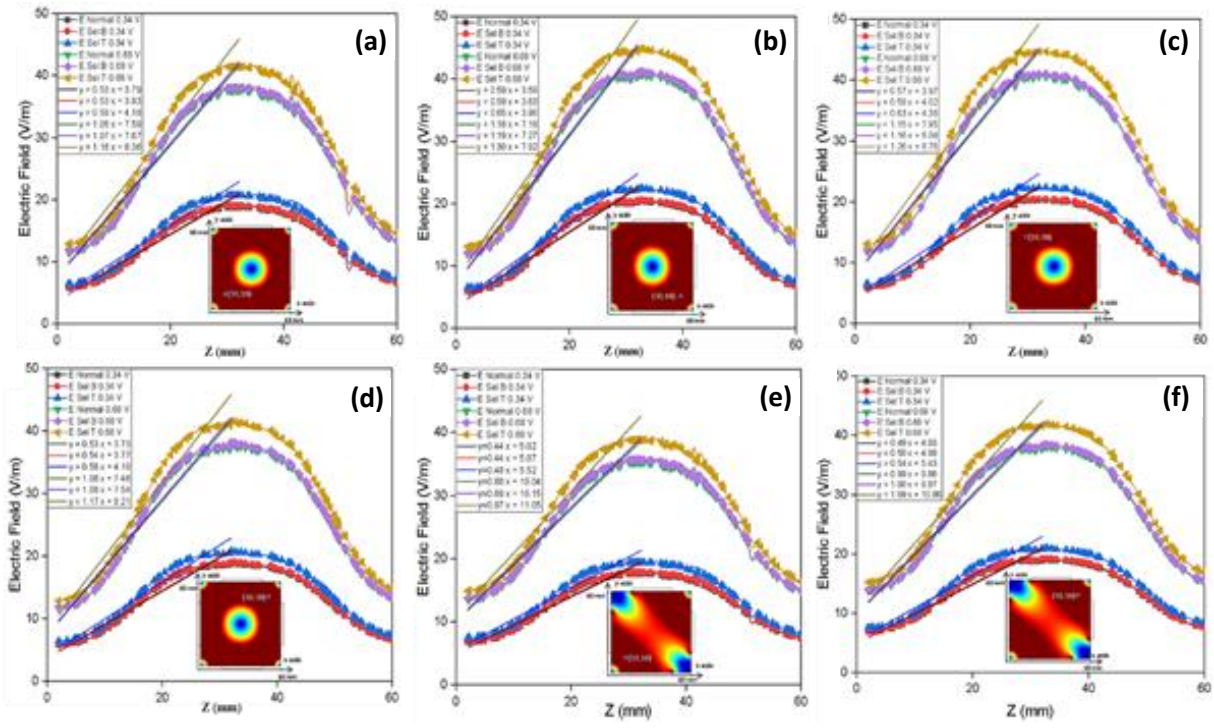


**Figure 5.** Graph of the electric field in the XY plane concerning the Z-axis, (a) coordinate point (10, 10) of model 2, (b) coordinates point (10, 50) of model 2, (c) coordinate point (50, 10) of model 2, (d) coordinate point (50, 50) of model 2, (e) coordinate point (10, 10) of model 1, and (f) coordinate point (50, 50) of model 1.

The gradient value in model 2 is above 0 for all mediums and input voltages, which means a positive slope occurs as the depth increases. At coordinates (10.10), the slope at a voltage of 0.34 V in normal blood medium, B cells, and T cells are 0.53; 0.53, and 0.58 respectively, while at the input voltage of 0.68 V, the slope is 1.06; 1.07 and 1.16. At coordinates (50.10), the slope at a voltage of 0.34 V on normal blood medium, B cells, and T cells are 0.59; 0.59, and 0.65, while at the input voltage of 0.68 V, the slope is 1.18; 1.19 and 1.30. At coordinates (10.50) the slope at a voltage of 0.34 V on normal blood medium, B cells, and T cells are 0.57; 0.58, and 0.63, while at the input voltage of 0.68 V, the slope is 1.15; 1.16, and 1.26. At coordinates (50.50) the slope at a voltage of 0.34 V on normal blood medium, B cells, and T cells are

0.53; 0.54, and 0.58, while at the input voltage of 0.68 V, the slope is 1.06, 1.08, and 1.17. There is a similarity of slope in the coordinates (10,10) with (50,50) and (50,10) with (10,50).

In model 1, at coordinates (10.10), the slope at a voltage of 0.34 V on normal blood medium, B cells, and T cells are 0.44; 0.44 and 0.48 respectively, while at the input voltage of 0.68 V, it is 0.88, 0.89 and 0.97. At coordinates (50.50) the slope at a voltage of 0.34 V on normal blood medium, B cells, and T cells are 0.49, 0.50, and 0.54, while at the input voltage of 0.68 V, it is 0.99, 1.00, and 1.00. There is a slight difference for the slope value in model 1 between the coordinates (10.10) and (50.50). In comparison between model 2 and model 1, the slope of model 2 has a higher value than model 1, hence the gradient value of the electric field for model 2 is greater than that of model 1. For the 0.68 V input voltage variation in model 2, the gradient value obtained is higher than 0.34 V, namely above 1 for the entire medium, hence model 2 with an input voltage of 0.68 V has a high electric field gradient, which indicates a high change in the electric field value with the position. At this point $\nabla|E^2|$ factor has a high value and allows a large electrophoretic force to occur.

After obtaining the electric field gradient at a certain point in the XY plane with a variation of the Z-coordinate, it is plotted on the Z-coordinate at Z = 30 mm along the X-axis and Y-axis at 3 points of 10 mm, 30 mm, and 50 mm with input voltage 0.68 V. This graph is used to determine the trend of the electric field along the X and Y-axis used to describe how well it moves the blast cell to approach the filter area near the electrode and be trapped there. Figure 6 shows the electric field graphs at 10 mm, 30 mm, and 50 mm points for the B-lymphocyte and T-lymphocyte medium along the X and Y-axis. It was found that the electric field at the 30 mm point had the best slope for B and T lymphocytes, hence in that area, the most optimal electrophoretic force was generated.

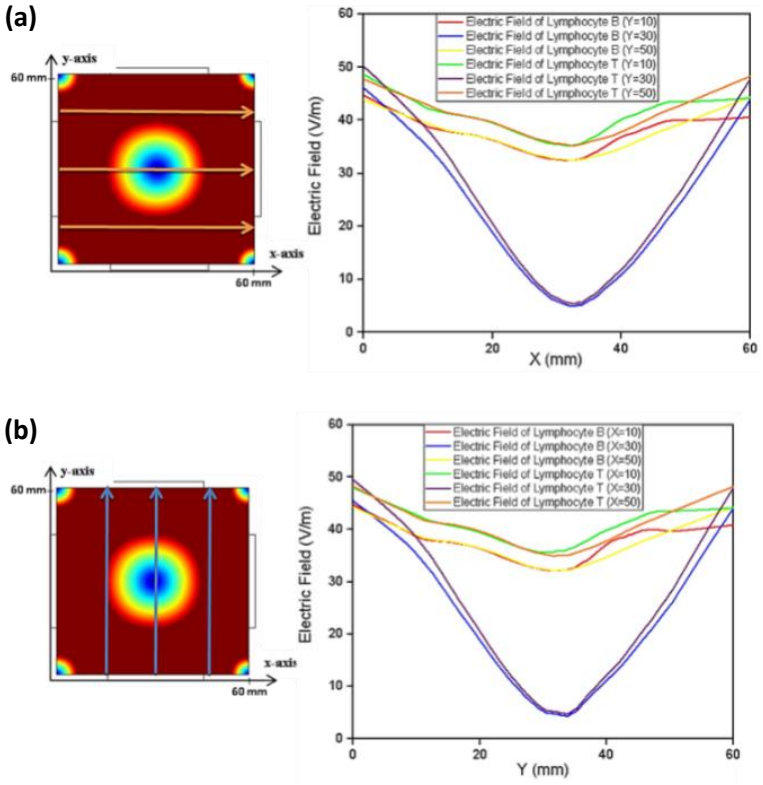


**Figure 6.** The distribution of the electric field at the Z-coordinate = 30 mm at several points X and Y with an input voltage of 0.68 V and B and T lymphocytes mediums: (a) along the X-axis at the point (0, 10); (0, 30) and (0, 50), and (b) along the Y-axis at the point (10, 0); (30, 0) and (50, 0)

Blood contains solid and liquid particles, 55% of blood is plasma, 90% of plasma is water. Furthermore, the remaining 45% of blood contains three types of cells namely, red blood cells (erythrocytes), white blood cells (leukocytes), and platelets [32].

Leukemia patients have many immature white blood cells known as blast cells, which are particles suspended in blood plasma, such that, the application of an electric field polarizes the particle into dipole molecules, and Coulomb interaction occurs between the dipole and the electric field. In a case where there is a non-uniform electric field, the net force moves the particle towards or against a high electric field intensity [33]. This leads to electroporation because of the high permittivity of the particle to that of the solvent [23]. White blood cells contain T Lymphocytes, B Lymphocytes, Monocytes, and Granulocytes with permittivity values of 103.9; 154.4; 126.8, and 150.9 respectively [34], and the permittivity of the solvent (water) is 88. Therefore, the white blood cells are suspended in the plasma and an electric field is applied, such that the phenomenon of positive electroporation occurs.

The dielectrophoretic force drives the bioparticles into a high-intensity electric field with the equation,

$$F_{DEP}=2\pi\varepsilon_m r^3 Re\,(f_{CM})\,\nabla\,|E^2| \quad (4)$$

where $r$ is the blast cell radius, $\varepsilon_m$ is the permittivity of the medium, $E$ is the electric field and $f_{CM}$ is the Claussius-Mossoti factor indicated by

$$f_{CM} = \frac{\varepsilon_p^* - \varepsilon_m^*}{\varepsilon_p^* + 2\varepsilon_m^*} \quad (5)$$

with $\varepsilon^*$ is the complex permittivity of $\left(\varepsilon^* = \varepsilon - \frac{i\,\sigma}{\omega}\right)$, $\sigma$ and $\omega$ are the conductivity as well as the angular frequency of the source, and $p$ and $m$ indexes indicate particle and medium. The Claussius-Mossoti factor of white blood cells suspended in water at various frequencies is obtained as shown in Figure 7. At a single frequency (100 kHz), the Claussius-Mossoti factor is positive, and the system applies a positive dielectrophoretic force such that the parameters other than the electric field divergence are constant. Therefore, resulting in the following equation.

$$F_{DEP} = C\,\nabla\,\left|E^2\right| \quad (6)$$

where C is a constant given by $C = 2\pi\varepsilon_m r^3$ the electrophoretic force is dominated by the electric field gradient. By knowing the distribution of the electric field, which enables knowing the gradient as the spatial coordinate changes.

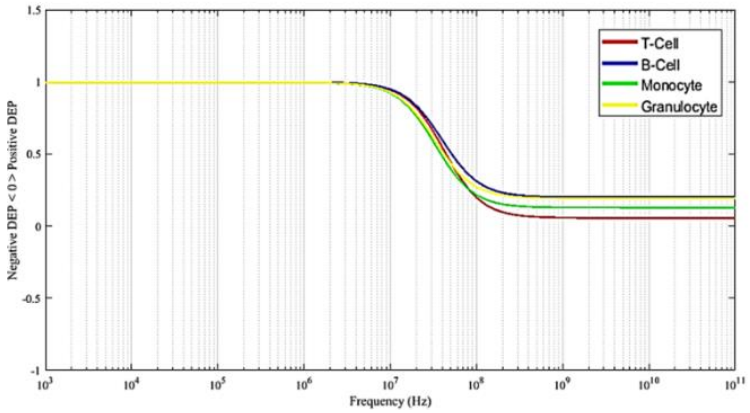


**Figure 7.** Claussius-Mossoti Factor of B Lymphocytes, T Lymphocytes, Monocytes, and Granulocytes suspended in water as measured at various frequencies

Changes in the electric field in spatial space, as in the 1-dimensional analysis for depth variations obtained the most optimal gradient at Z = 30 mm. While for variations of the X coordinates at 3 points namely, Y (10,30 and 50), the optimal gradient was obtained at Y = 30 mm, as well as the variation of the Y coordinate at 3 points namely, X (10,30 and 50) with an optimal gradient at X = 30 mm. In other words, at a 30 mm depth of Z, X, and Y points, the optimal electrophoretic force occurs in the direction of the electrode, as illustrated in Figure 8.

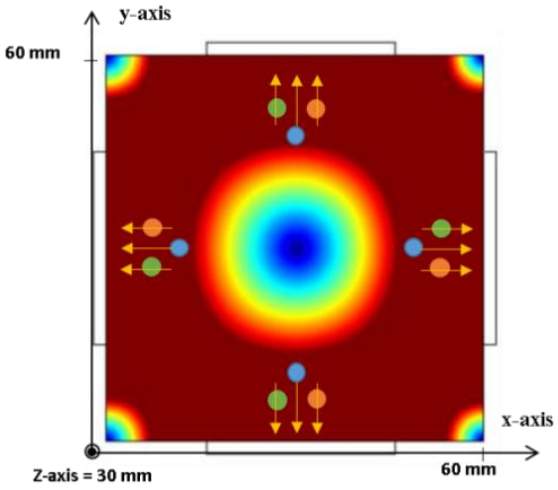


**Figure 8.** Illustration of the electrophoretic force direction of blood particles on a 4-electrode system

## CONCLUSION

Differences in the arrangement of the electrodes cause changes in the electric field distribution, which was obtained in model 2 with an input voltage of 0.68 V. The electrophoretic force depends on the electric field gradient, and at the XY coordinate point with the Z-coordinate variation, the highest gradient is obtained at the coordinates (10.10), (10.50), (50.10) and (50.50) in model 2, while in model 1 it is obtained at points (10.10) and (50.50), and the optimal Z-coordinate is obtained at Z = 30 mm. Furthermore, along the X-axis and Y-axis, the highest gradient was obtained at a point of 30 mm, both in the B and T lymphocytes medium with an input voltage of 0.68 V. Consequently, the most optimal model for making electrophoretic force is model 2, at spatial position Z = 30 mm with the X-axis and Y-axis at the point 30 mm which is also known to be the center of the model. In a situation where an alternating electric field is applied, the cells undergo positive electrophoresis which moves the particles towards an area of high intensity near the electrodes and allows the particles to accumulate such that, the filter placement is being conducted in that area.

## ACKNOWLEDGEMENT

The authors gratefully acknowledge finan-cial support from the Institut Teknologi Sepuluh Nopember and BRIN-RISTEK DIKTI under Basic (PD) (No. 802/PKS/ITS/2021) for this work, under the project scheme of the Publication Writing and IPR Incentive Program (PPHKI).

## REFERENCES

[1] N. C. Institute, "Cancer Stat Facts: Leukemia", *National Cancer Institute*, 2021.
[2] D. Rodriguez-Abreu, A. Bordoni, and E. Zucca, "Epidemiology of hematological malignancies", *Annals of Oncology*, vol. 18, no. SUPPL. 1, pp. 13–18, 2007.
[3] A. M. and A. M. Janjua H U, Naeem K, "Rouleaux formation of white blood cells and platelets in leukemia", *Bioscience Journal*, vol. 34, no. 2, pp. 1010–20, 2018.
[4] T. A. Crowley and V. Pizziconi, "Isolation of plasma from whole blood using planar microfilters for lab-on-a-chip applications", *Lab on a Chip*, vol. 5, no. 9, pp. 922–929, 2005.
[5] H. M. Ji, V. Samper, Y. Chen, C. K. Heng, T. M. Lim, and L. Yobas, "Silicon-based microfilters for whole blood cell separation", *Biomedical Microdevices*, vol. 10, no. 2, pp. 251–257, 2008.
[6] S. Ferdowsi, Z. Abbasi-Malati, and A. A. Pourfathollah, "Leukocyte reduction filters as an alternative source of peripheral blood leukocytes for research", *Hematology, Transfusion and Cell Therapy*, no. x x, pp. 0–4, 2021.
[7] K. Sriprawat *et al.*, "Effective and cheap removal of leukocytes and platelets from plasmodium vivax infected blood", *Malaria Journal*, vol. 8, no. 1, pp. 1–7, 2009.
[8] S. Larsson, H. Gulliksson, and D. Paunovic, "Evaluation of a whole-blood WBC-reduction filter that saves platelets: In vitro studies", *Transfusion*, vol. 41, no. 4, pp. 534–539, 2001.
[9] V. Fahradyan *et al.*, "Leukoreduction in ex vivo perfusion circuits: comparison of leukocyte depletion efficiency with leukocyte filters", *Perfusion (United Kingdom)*, vol. 35, no. 8, pp. 853–860, 2020.
[10] G. Rozenberg, *Microscopic 3e Heamotology a Practical guide for the laboratory*. 2011.
[11] O. Z. Siani, M. Sojoodi, M. Z. Targhi, and M. Movahedin, "Blood particle separation using dielectrophoresis in a novel microchannel: A numerical study", *Cell Journal*, vol. 22, no. 2, pp. 218–226, 2019.
[12] C. Szydzik, K. Khoshmanesh, A. Mitchell, and C. Karnutsch, "Microfluidic platform for separation and extraction of plasma from whole blood using dielectrophoresis", *Biomicrofluidics*, vol. 9, no. 6, pp. 1–16, 2015.
[13] I. Doh and Y. H. Cho, "A continuous cell separation chip using hydrodynamic dielectrophoresis (DEP) process", *Sensors and Actuators, A: Physical*, vol. 121, no. 1, pp. 59–65, 2005.
[14] M. Jahangiri *et al.*, "Low frequency stimulation induces polarization-based capturing of normal, cancerous and white blood cells: A new separation method for circulating tumor cell enrichment or phenotypic cell sorting", *Analyst*, vol. 145, no. 23, pp. 7636–7645, 2020.
[15] D. W. Lee and Y. H. Cho, "A continuous electrical cell lysis device using a low dc voltage for a cell transport and rupture", *Sensors and Actuators, B: Chemical*, vol. 124, no. 1, pp. 84–89, 2007.
[16] C. Kremer, C. Witte, S. L. Neale, J. Reboud, M. P. Barrett, and J. M. Cooper, "Shape-dependent optoelectronic cell lysis", *Angewandte Chemie - International Edition*, vol. 53, no. 3, pp. 842–846, 2014.
[17] Y. Palti, "Method for Selectively Destroying Dividing Cells", U.S. Patent Application No, 11/470,405, 2007.
[18] C. Polk, "Therapeutic applications of low-frequency sinusoidal and pulsed electric and magnetic fields", in *Bronzino J D, editor The biomedical engineering handbook.*, 1995, pp. 1404–16.
[19] C. A. L. Bassett, "The development and application of pulsed electromagnetic fields (PEMFs) for ununited fractures and arthrodeses", *Clin Plast Surg*, vol. 12, no. 2, pp. 259–77, 1985.
[20] E. Elson, "Biologic effects of radiofrequency and microwave fields: in vivo and in vitro experimental results.", in *In: Bronzino JD, editor. The biomedical engineering handbook*, 1995, pp. 1417–23.
[21] E. D. Kirson, R. S. Schneiderman, V. Dbaly, F. Tovarys, J. Vymazal, A. Itzhaki, M. Daniel, G. Zoya, S. Esther, G. Dorit, W. Yoram W, and Y. Palti, "Chemotherapeutic Treatment Efficacy and Sensitivity are Increased by Adjuvant Alternating Electric Fields (TTFields)", *BMC Med.Phys*, vol. 9, no. 1, pp. 1–13, 2009.

[22] S. Takashima and H. P. Schwan, "Alignment of microscopic particles in electric fields and it's biological implications", *Biophys J*, vol. 47, no. 4, pp. 513–518, 1985.
[23] Y. Huang and R. Pethlg, "Electrode design for negative dielectrophoresis", *Measurement Science and Technology*, vol. 2, no. 12, pp. 1142–1146, 1991.
[24] A. R. and N. N. Miftakhul Firdhaus, Ulya Farahdina, Vinda Zakiyatuz Zulfa, Endarko, "Electric Field Distribution Analysis of Blood Cancer as a Potentially Blood Cancer Therapy", 2021.
[25] IFAC, "Calculation of the Dielectric Properties of Body Tissues in the frequency range 10 Hz - 100 GHz", *Italian National Research Council*, 2021.
[26] A. Surowiec, S. S. Stuchly, and C. Izaguirre, "Dielectric properties of human B and T lymphocytes at frequencies from 20 kHz to 100 MHz", *Physics in Medicine and Biology*, vol. 31, no. 1, pp. 43–53, 1986.
[27] G. A. Justin, Y. Zhang, X. T. Cui, C. W. Bradberry, M. Sun, and R. J. Sclabassi, "A Metabolic Biofuel Cell: Conversion of Human Leukocyte Metabolic Activity to Electrical Currents", *Journal of Biological Engineering*, vol. 5, no. 1, p. 5, 2011.
[28] B. A. Markx, L. Carney, M. Littlefair, and A. Sebastian, "Recreating the hematon Microfabrication of artificial haematopoietic stem cell micronichesin vitrousing dielectrophoresis", *Biomed Microdevices*, vol. 11, no. 1, pp. 143–150, 2009.
[29] D. S. Gray, J. L. Tan, J. Voldman, and C. S. Chen, "Dielectrophoretic registration of living cells to a microelectrode array", *Biosens Bioelectron*, vol. 19, no. 12, pp. 1765–1774, 2004.
[30] M. Schueller, A. Blaszczyk, F. Mauseth, H. K. Meyer, N. Stieger, and J. Smajic, "Charge Accumulation on Slightly Conductive Barrier Systems and Its Effect on Breakdown Voltage in an Air Insulated Rod Plane", in *Arrangement Proceedings of the 21st International Symposium on High Voltage Engineering*, 2020, pp. 1155–1165.
[31] A. B. and H. M. Hazlee I, Mohsin AT, "Distribution of electric field in capacitor and surge arrester bushings", *IEEE International Conference on Power and Energy (PECon)*, pp. 973–978, 2012.
[32] P. S, *The Concise Human Body book*. 2019.
[33] T. B. Jones and T. B. Jones, "Electromechanics of particles", in *Cambridge University Press*, 2005, 26, pp. 1780-1789.
[34] J. Yang, Y. Huang, X. Wang, X. B. Wang, F. F. Becker, and P. R. Gascoyne, "Dielectric Properties of Human Leukocyte Subpopulations Determined by Electrorotation as a Cell Separation Criterion", *Biophysical Journal*, vol. 76, no. 6, pp. 3307–3314, 1999.